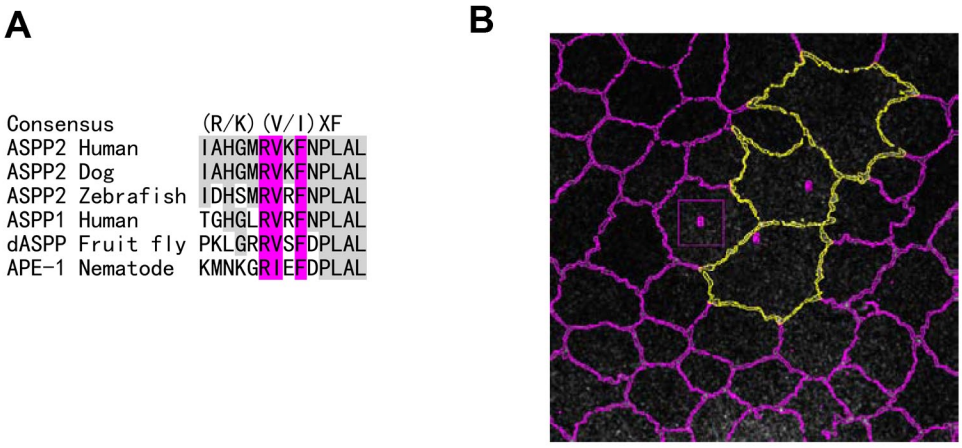


**Figure S1. Yamashita K et al.**

**Fig. S1. Related to Fig. 1.** (A) Sequence alignment of the PP1-binding consensus sequence in ASPP2 and its homologs. Magenta indicates the consensus PP1-binding sequence. (B) Optical sections were obtained at 0.4-µm intervals by confocal microscopy. Among sections, ZO-1-positive sequential four slices were projected. A tight junction region was defined by thresholding and binarizing ZO-1-staining (magenta). By manual deletion of a V5-negative region, ROI was generated (yellow). Relative intensity was calculated by dividing [mean of magenta] by [mean of yellow]. A background signal was subtracted for quantification.

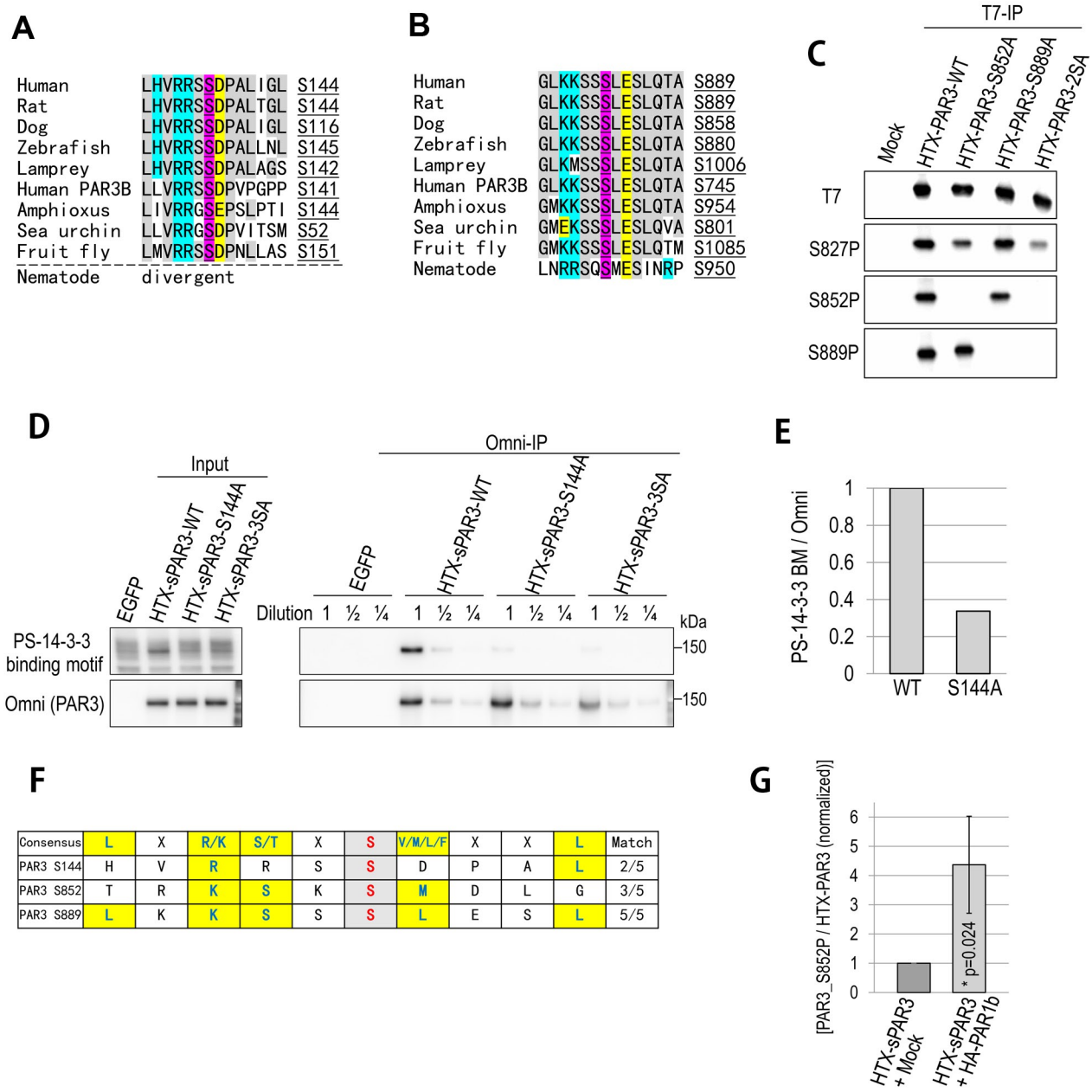


## Figure S2. Yamashita K et al.

**Fig. S2. Related to Fig. 2.** (A) Sequence alignment around Ser144 of PAR3. (B) Sequence alignment around Ser889 of PAR3. (C) PAR3 and its point mutants were exogenously expressed in MDCK cells and immunoprecipitated. Specificity of phosphorylated serine-specific antibodies was confirmed by western blotting. (D) His-T7-Xpress-tagged wild-type PAR3, PAR3-S144A, and PAR3-3SA (S144A/S852A/S889A) were exogenously expressed in MDCK cells and immunoprecipitated. Then, western blotting was performed. The 14-3-3-binding motif antibody primarily recognized the phosphorylation of Ser144 in PAR3. (E) Quantification of the signal using 14-3-3-binding motif antibody. Signal intensity was normalized by total HTX-PAR3 (Omni). (F) The consensus sequence of the PAR1 substrate and the sequence around S144, S852, and S889 of PAR3. (G) PAR1b overexpression-mediated phosphorylation of Ser852 of PAR3 was quantified.

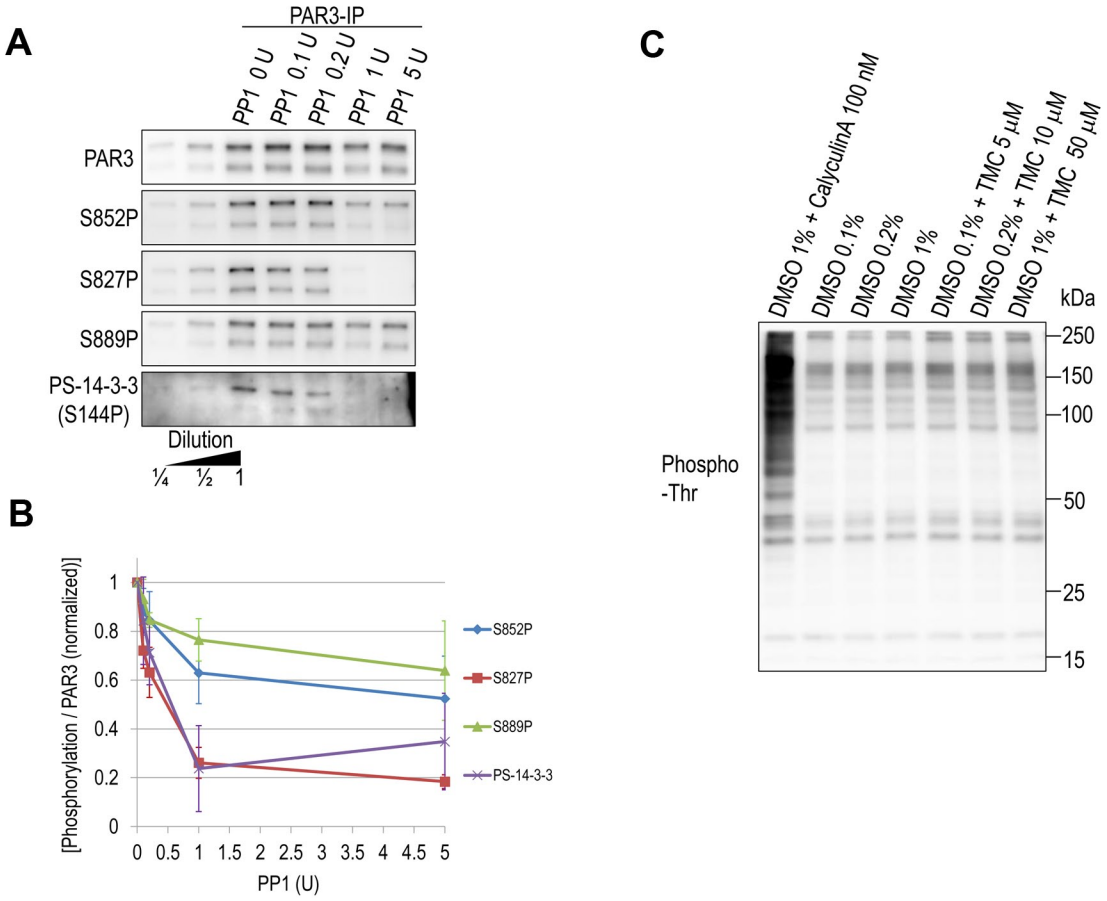


## Figure S3. Yamashita K et al.

**Fig. S3. Related to Fig. 3.** (A) PAR3 was immunopurified from MDCK cells, and recombinant PP1α was treated. After incubation, the phosphorylation levels were assayed by western blotting. (B) Quantification of PAR3 phosphorylation in experiment A (n = 3). (C) MDCK cells were treated with the broad phosphatase inhibitor calyculin A and the PP1-specific inhibitor tautomycetin (TMC) for 1 h using DMSO as a vehicle. Calyculin A broadly promoted a variety of protein phosphorylation, whereas the effect of tautomycetin appeared to be confined.

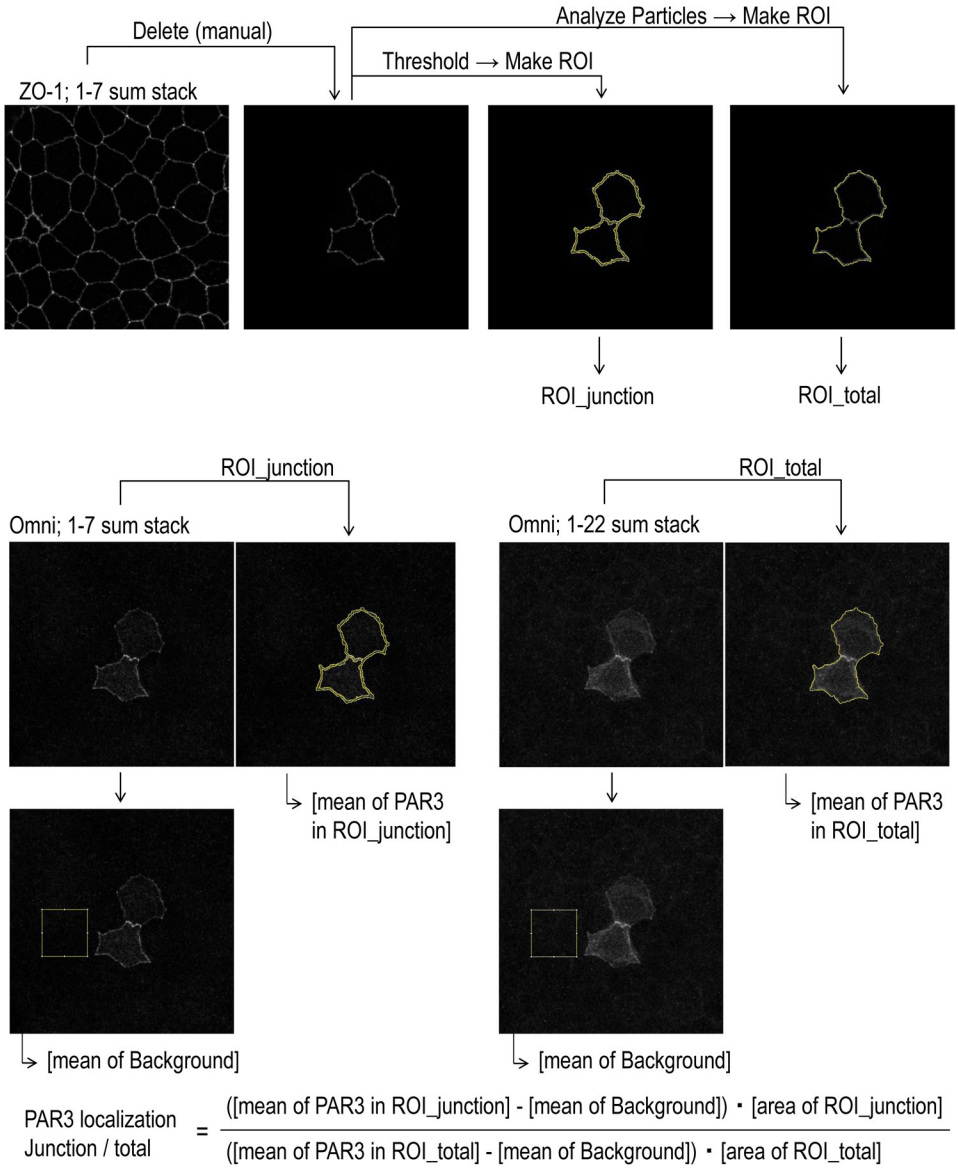


## Figure S4. Yamashita K et al.

**Fig. S4. Related to Fig. 4.** Optical sections were obtained at 0.4-μm intervals by confocal microscopy. Among sections, ZO-1-positive sequential sections were projected. A tight junction region was defined by thresholding and binarizing ZO-1-staining. After deleting Omni-negative cells, ROI was generated (ROI_junction). On the other hand, ROI_total was generated by applying analyze particle tool to z-projection of ZO-1-staining. For quantification, the background signal was subtracted.

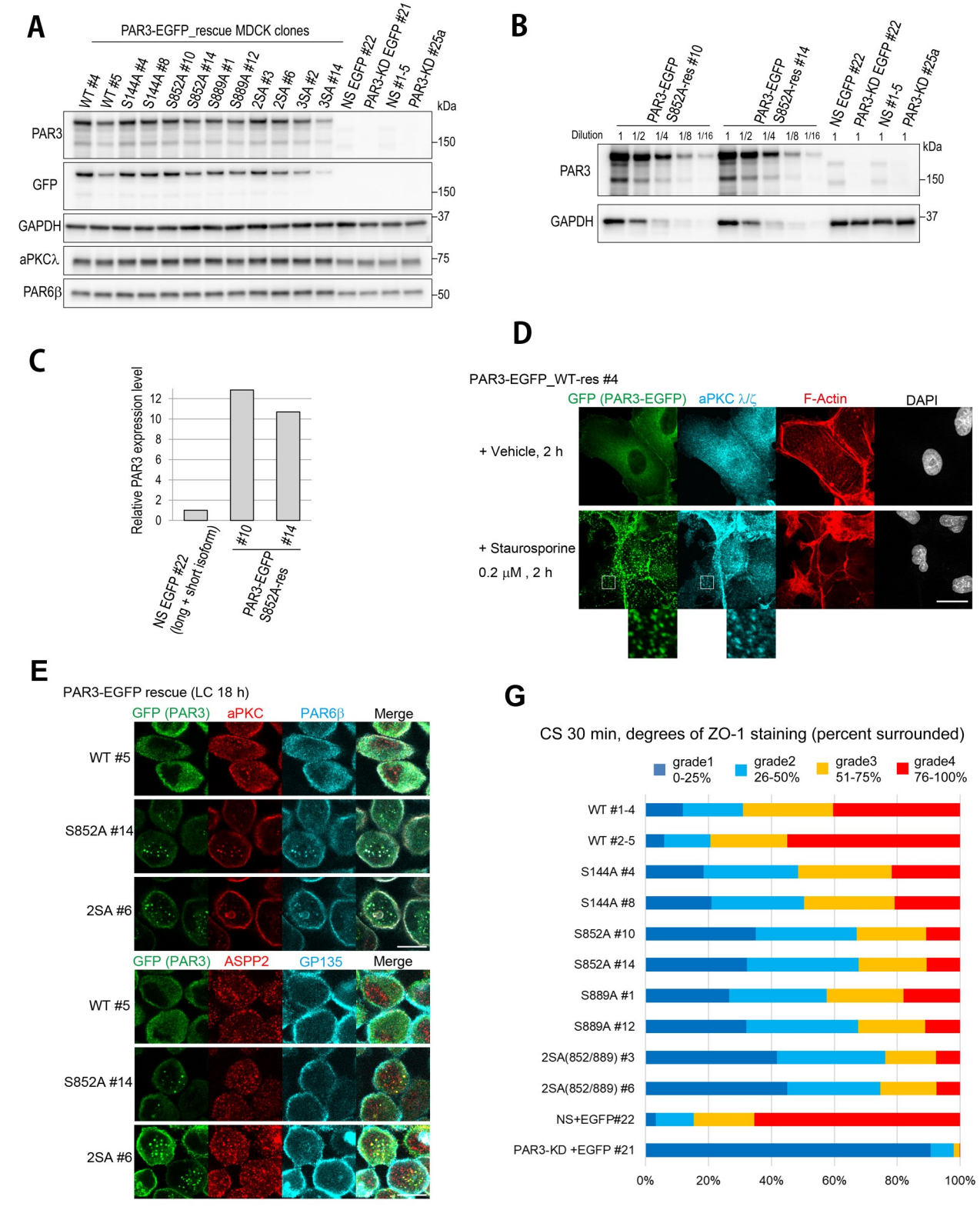


**Figure S5. Yamashita K et al.**

**Fig. S5. Related to Fig. 5.** (A) Expression levels of PAR3-EGFP in PAR3-rescued cells. Whole cell lysates of indicated cell lines were analyzed. 10 μg/lane of proteins was used. 2SA and 3SA indicate S852A/S889A double-mutant and S144A/S852A/S889A triple-mutant, respectively. (B) Whole cell lysates of PAR3-EGFP-S852A-rescued cells were diluted and compared to the endogenous level. (C) Densitometric analysis of the result in (B). Signals from endogenously expressed long and short PAR3 isoforms were integrated. (D) PAR3-WT-EGFP-rescued cells were treated with 0.2 μM staurosporine for 2 h. Punctate staining of PAR3-EGFP and aPKC was evident by staurosporine treatment. (E) PAR3-rescued MDCK cell lines were cultured in low-calcium medium for 18 h. Then, immunofluorescence staining was performed. One confocal section is displayed. (F) After 2 h of calcium switch, immunofluorescence staining was performed. The MIP of immunofluorescent confocal sections is displayed. (G) After 30 min of calcium switch, ZO-1-staining was evaluated as an indicator of tight junction maturation. Degrees of surrounding ZO-1-staining are indicated by colors. Cell populations are represented with length of bars (average of three independent experiments). Scale bars represent 20 μm.

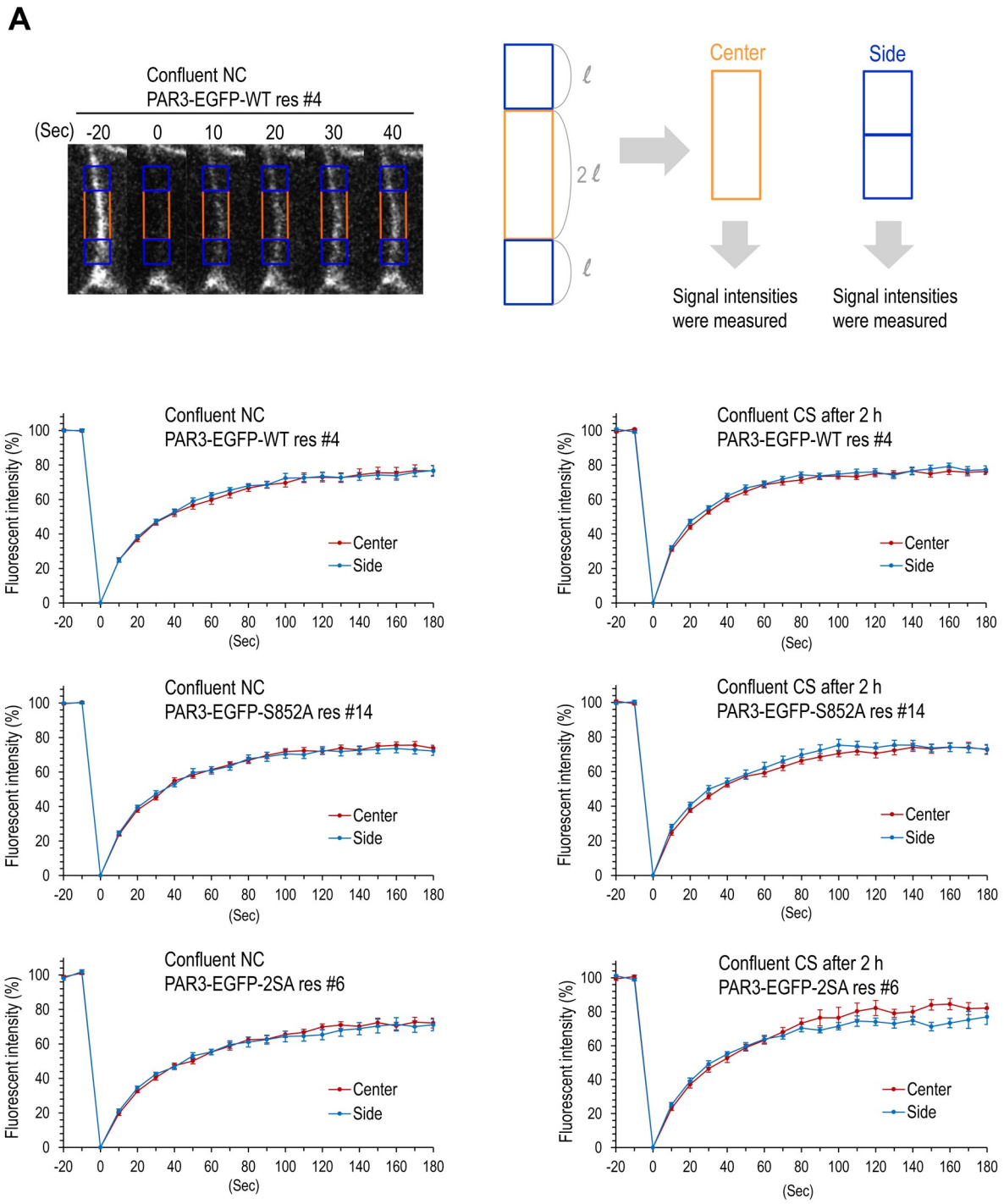


**Figure S6. Yamashita K et al.**

**Fig. S6. Related to Fig. 6.** (A) The fluorescent recovery adjacent to unbleached membrane region (side) and that in distal region (center) were compared. Uniform recovery was observed in each PAR3-rescued line and both culture conditions. (B, C) PAR3-EGFP-rescued cell lines were confluently cultured in normal calcium medium and subjected to FRAP assay. Average values of mobile fraction and half time of recovery were plotted. Residual transformant clones were used, which were not used in Fig. 6. Student's t-test was used for statistical analysis; each PAR3 mutant-rescued line was compared with PAR3 wild-type-rescued #5. Error bars represent ± standard error (SE).

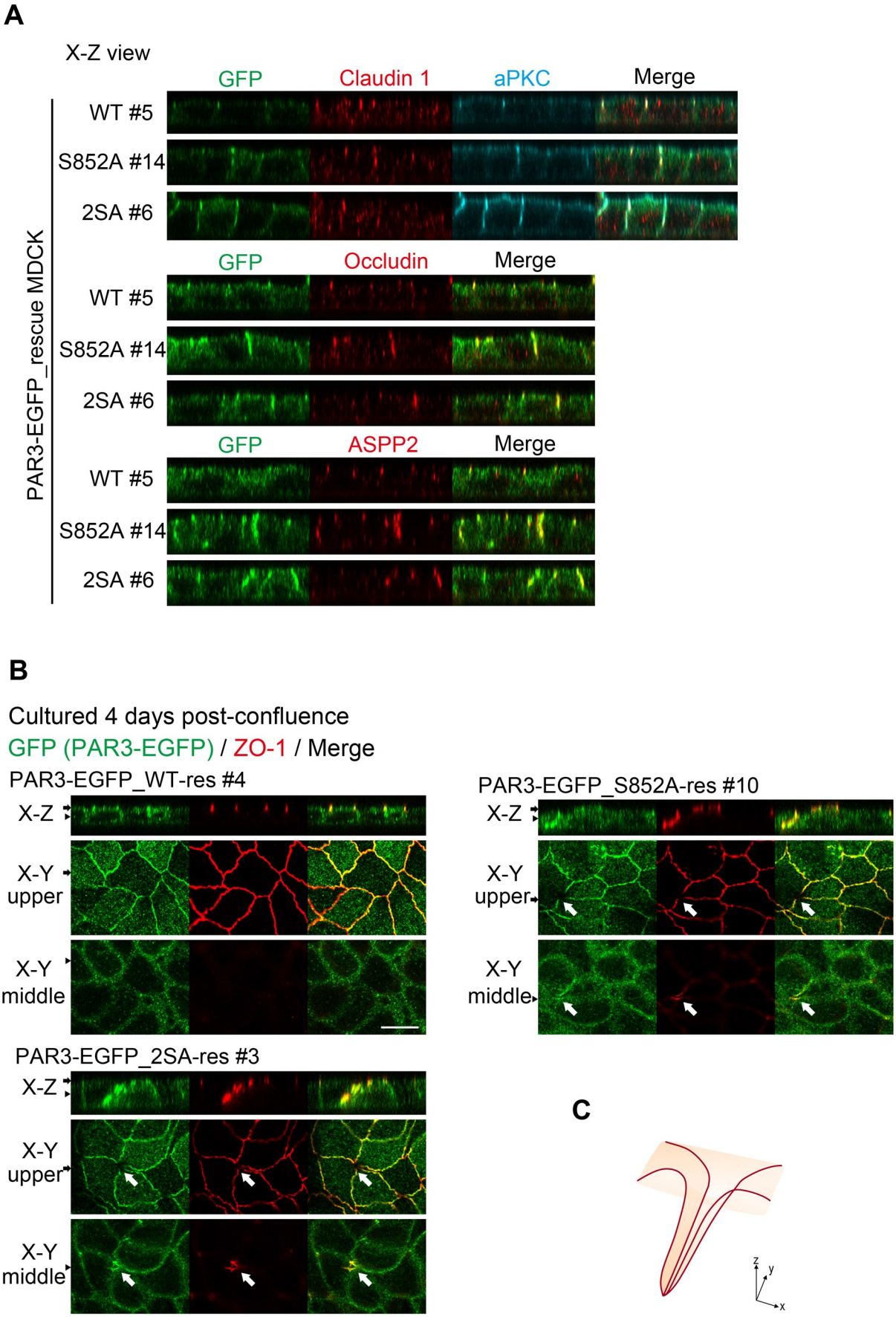


**Figure S7. Yamashita K et al.**

**Fig. S7. Related to Fig. 7.** (A) PAR3-rescued cell lines were cultured for 4 days (reached confluence at day 2). Immunostained samples were analyzed by confocal microscopy, and reconstituted X–Z sections are shown. Tight junction components were partially colocalized with unphosphorylatable PAR3 mutants at the lateral membrane domains. (B) PAR3-rescued cell lines were cultured for 6 days (reached confluence at day 2). Immunostained samples were analyzed by confocal microscopy. Black arrows and arrowheads are placed in the same manner as in Fig. 7A. White arrows indicate tubular invaginations. (C) Expected 3D structure of the tubular invaginations. Lines represent tight junctions.

Table S1. List of antibodies used in this study.

| Antibodies | Host | Source | Cat# | Application/Dillution |
|---|---|---|---|---|
| anti-PAR3 | Rabbit | Upstate (Merck) | 07-330 | WB (1:500), IF (1:300), IP (2μg) |
| anti-phospho-PAR3 Ser827 | Rabbit | Nagai-Tamai et al., 2002 | N/A | WB (1:300) |
| anti-phospho-PAR3 Ser852 | Rabbit | This study | N/A | WB (1:100) |
| anti-phospho-PAR3 Ser889 | Rabbit | This study | N/A | WB (1:500) |
| anti-ASPP2 | Rabbit | Cong et al., 2010 | N/A | WB (1:1000), IF (1:1000) |
| anti-PP1α | Mouse | Santa Cruz Biotechnology | sc-7482 | WB (1:200) |
| anti-PP2A C subunit | Mouse | Upstate (Merck) | 05-421 | WB (1:1000) |
| anti-aPKC | Rabbit | Santa Cruz Biotechnology | sc-216 | WB (1:1000), IF (1:300) |
| anti-aPKC | Mouse | BD BioSciences | 610176 | WB (1:1000) |
| anti-phospho-aPKCζ Thr410 | Rabbit | Cell Signaling Technology | 9378 | WB (1:500) |
| anti-PAR6β | Rabbit | Santa Cruz Biotechnology | sc-67392 | WB (1:1000), IF (1:500) |
| anti-pan 14-3-3 | Rabbit | Santa Cruz Biotechnology | sc-629 | WB (1:1000) |
| anti-ZO-1 | Rat | Santa Cruz Biotechnology | sc-33725 | IF (1:300) |
| anti-claudin1 | Rabbit | Zymed (Thermo Fisher Scientific) | 71-7800 | IF (1:200) |
| anti-occludin | Rabbit | Zymed (Thermo Fisher Scientific) | 71-1500 | IF (1:200) |
| anti-E-cadherin | Mouse | BD BioSciences | 610181 | IF (1:500) |
| anti-myosin light chain 2 | Rabbit | Cell Signaling Technology | 3672 | WB (1:500) |
| anti-phospho-myosin light chain 2 | Rabbit | Cell Signaling Technology | 3674 | WB (1:500) |
| anti-phospho-Ser 14-3-3-binding motif | Mouse | Cell Signaling Technology | 9606 | WB (1:100) |
| anti-phospho-threonine | Mouse | Cell Signaling Technology | 9386 | WB (1:1000) |
| anti-V5 | Mouse | Invitrogen (Thermo Fisher Scientific) | R960-25 | WB (1:1000), IF (1:500), IP (2μg) |
| Omni probe (anti-His-T7-Xpress-tag) | Mouse | Santa Cruz Biotechnology | sc-7270 | WB (1:1000), IF (1:300) |
| Omni probe (anti-His-T7-Xpress-tag) | Rabbit | Santa Cruz Biotechnology | sc-499 | WB (1:1000), IP (2μg) |
| anti-T7 | Mouse | Novagen (Merck) | 69522 | WB (1:5000), IP (2μg) |
| anti-GFP | Rabbit | MBL | 598 | WB (1:1000) |
| anti-GFP | Chick | aves Labs | GFP-1010 | IF (1:5000) |
| anti-HA (3F10) | Rat | Roche (Merck) | 11867423001 | WB (1:500) |
| anti-GST | Rabbit | Izumi et al., 1998 | N/A | WB (1:1000) |
| anti-GAPDH | Mouse | abcam | ab8245 | WB (1:200000) |
| anti-YAP1 | Mouse | Abnova | H00010413-M01 | WB (1:1000) |
| Normal rabbit IgG | Rabbit | Santa Cruz Biotechnology | sc-2027 | IP (2μg) |